

Domain Switching Kinetics in Disordered Ferroelectric Thin Films

J. Y. Jo,¹ H. S. Han,¹ J.-G. Yoon,² T. K. Song,³ S.-H. Kim,⁴ and T. W. Noh^{1,*}

¹ReCOE&FPRD, Department of Physics and Astronomy, Seoul National University, Seoul 151-747, Korea

²Department of Physics, University of Suwon, Suwon, Gyeonggi-do 445-743, Korea

³School of Nano Advanced Materials, Changwon National University, Changwon, Gyeongnam 641-773, Korea

⁴R&D center, Inostek Inc., Ansan, Gyeonggi-do 426-901, Korea

(Dated: February 1, 2008)

We investigated domain kinetics by measuring the polarization switching behaviors of polycrystalline $\text{Pb}(\text{Zr},\text{Ti})\text{O}_3$ films, which are widely used in ferroelectric memory devices. Their switching behaviors at various electric fields and temperatures could be explained by assuming the Lorentzian distribution of domain switching times. We viewed the switching process under an electric field as a motion of the ferroelectric domain through a random medium, and we showed that the local field variation due to dipole defects at domain pinning sites could explain the intriguing distribution.

PACS numbers: 77.80.Fm, 77.80.Dj, 77.84.Dy

Domain switching kinetics in ferroelectrics (FEs) under an external electric field E_{ext} have been extensively investigated for several decades [1, 2, 3, 4, 5, 6, 7, 8, 9]. The traditional approach to explain the FE switching kinetics, often called the Kolmogorov-Avrami-Ishibashi (KAI) model, is based on the classical statistical theory of nucleation and unrestricted domain growth [10, 11]. For a uniformly polarized FE sample under E_{ext} , the KAI model gives the time (t)-dependent change in polarization $\Delta P(t)$ as

$$\Delta P(t) = 2P_s[1 - \exp\{-(t/t_0)^n\}], \quad (1)$$

where n and t_0 are the effective dimension and characteristic switching time for the domain growth, respectively, and P_s is spontaneous polarization. When the nuclei are appearing in time with the same probability, $n = 3$ for bulk samples and $n = 2$ for thin films [12]. In addition, t_0 is proportional to the average distance between the nuclei, divided by the domain wall speed. Several studies have used the KAI model successfully to explain the $\Delta P(t)$ behaviors of FE single crystals and epitaxial thin films [2].

Recently, FE thin films have been intensively investigated for FE random access memory (FeRAM) [1]. Most commercial FeRAM use polycrystalline $\text{Pb}(\text{Zr},\text{Ti})\text{O}_3$ (poly-PZT) films, and their $\Delta P(t)$ behaviors determine the reading and writing speeds of the FeRAM. In such non-epitaxial FE films, a domain cannot propagate indefinitely due to pinning caused by numerous defects, so the KAI model cannot be applied. Therefore, it is important both scientifically and technologically to clarify the domain switching kinetics of polycrystalline FE films.

Numerous studies have examined the $\Delta P(t)$ behaviors of polycrystalline FE films, and the reported results vary markedly [3, 4, 5, 6, 7]. Lohse *et al.* measured the polarization switching currents of poly-PZT films, and showed that $\Delta P(t)$ slowed significantly compared to Eq. (1) [3]. Tagantsev *et al.* observed similar phenomena for poly-PZT films. To explain these behaviors, they developed

the nucleation-limited-switching (NLS) model. They assumed that films consist of several areas that have independent switching kinetics:

$$\Delta P(t) = 2P_s \int_{-\infty}^{\infty} [1 - \exp\{-(t/t_0)^n\}] F(\log t_0) d(\log t_0), \quad (2)$$

where $F(\log t_0)$ is the distribution function for $\log t_0$ [4]. They assumed a very broad mesa-like function for $F(\log t_0)$, and could explain their $\Delta P(t)$ data. The same

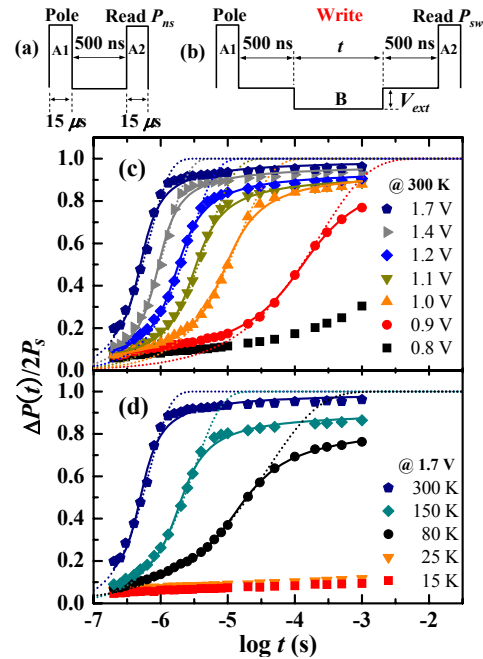


FIG. 1: (color online). Schematic diagrams of the pulse trains used to measure (a) non-switching polarization (P_{ns}) and (b) switching polarization (P_{sw}). Time (t)-dependent switched polarization $\Delta P(t)$ (c) under various external voltages (V_{ext}) at room temperature and (d) under 1.7 V at various temperatures. The dotted and solid lines correspond to fitted results using the KAI model and the Lorentzian distribution function in $\log t_0$, respectively.

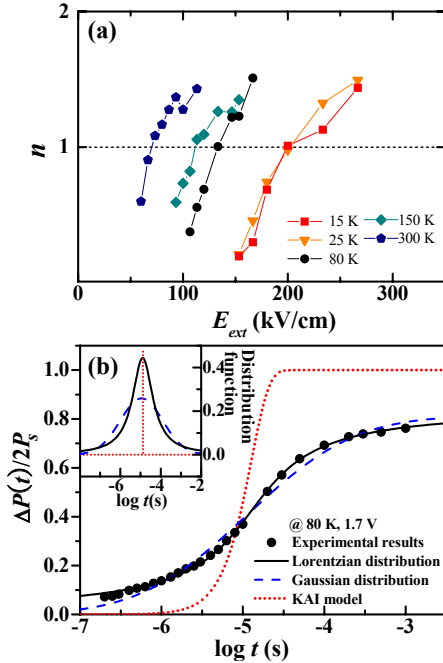


FIG. 2: (color online). (a) Values of n for various T and E_{ext} . (b) $\Delta P(t)$ results for (solid symbols) experimental data and fitted results using the Lorentzian (solid line), Gaussian (dashed line), and delta (dotted line) distributions for $\log t_0$. The inset shows the distribution functions corresponding to the fitted results.

authors also studied La-doped poly-PZT films and found that $\Delta P(t)$ at room temperature is limited mainly by nucleation, while at a low temperature (T), the switching kinetics are governed by domain wall motion, implying the validity of the KAI model [5].

In this Letter, we investigate the polarization switching behaviors of poly-PZT films. We can explain the measured $\Delta P(t)$ in terms of the Lorentzian distribution function for $F(\log t_0)$, irrespective of T . We show that such distribution arises from local field variation in a disordered system with dipole-dipole interactions.

Note that (111)-oriented poly-PZT films with a Ti concentration near 0.7 are the most widely used material in FeRAM applications. We prepared our polycrystalline $\text{PbZr}_{0.3}\text{Ti}_{0.7}\text{O}_3$ thin film on Pt/Ti/SiO₂/Si substrates using the sol-gel method. The poly-PZT film had a thickness of 150 nm. X-ray diffraction studies showed that it has the (111)-preferred orientation, and scanning electron microscopy studies indicated that our poly-PZT film consists of grains with a size of about 200 nm. We deposited Pt top electrodes using sputtering with a shadow mask. The areas of the top electrodes were about $7.9 \times 10^{-9} \text{ m}^2$.

We obtain the $\Delta P(t)$ values of our Pt/PZT/Pt capacitors using pulse measurements [2, 4, 13, 14]. Figure 1(a) shows the pulse trains used to measure the non-switching polarization change (P_{ns}). Using pulse A1, we

poled all the FE domains in one direction. Then, we applied pulse A2 with the same polarity, and measure the current passing a sensing resistor. By integrating the current, we could obtain the P_{ns} values. Figure 1(b) shows the pulse trains used to measure the switching polarization (P_{sw}). Inserting pulse B with the opposite polarity between pulses A1 and A2, we could reverse some portion of the FE domains, so the difference between the values of P_{sw} and P_{ns} represents the polarization change due to domain switching, namely $\Delta P(t)$. We varied t from 200 ns to 1 ms, and V_{ext} from 0.8 to 4 V. The value of E_{ext} can be estimated easily by dividing V_{ext} by the film thickness. At T of 80~300 K, we used pulses A1 and A2 with a height of 4 V, which was larger than the coercive voltage. Below 80 K, the coercive voltage increases, so we increased the pulse height to 6 V [15].

Figure 1(c) shows the values of $\Delta P(t)/2P_s$ at room temperature with numerous values of V_{ext} . Figure 1(d) shows the values of $\Delta P(t)/2P_s$ at various T with $V_{ext} = 1.7$ V. The dotted lines in both figures are the curves best fitting Eq. (1). The KAI model predictions deviated markedly from the experimental $\Delta P(t)$ values in the late switching stage, in agreement with Gruverman *et al.* [6]. In addition, the best fitting results with the KAI model gave unreasonable values of n . As shown in Fig. 2(a), the values of n varied markedly with T and E_{ext} . In addition, in the low E_{ext} region, we obtained n values much smaller than 1, which are not proper as an effective dimension of domain growth. Therefore, Eq. (1) fails to describe the polarization switching behaviors of our PZT films.

To explain the measured $\Delta P(t)$, we tried simple functions for $F(\log t_0)$ in Eq. (2). The opposite domain, once nucleated, will propagate inside the film, so we fixed $n=2$. The solid circles in Fig. 2(b) show the experimental $\Delta P(t)$ at 80 K with $V_{ext} = 1.7$ V. For $F(\log t_0)$, we tried the delta, Gaussian, and Lorentzian distribution functions, as shown in the inset. The dotted line indicates the fitting results using Eq. (2) with a delta function. Note that this curve corresponds to a fit with the KAI model, and thus the classical theory cannot explain our experimental data. The dashed line shows the Gaussian fitting results. Although this fitting seems reasonable, some discrepancies occur. The solid black shows the fitting results with the Lorentzian distribution:

$$F(\log t_0) = \frac{A}{\pi} \left[\frac{w}{(\log t_0 - \log t_1)^2 + w^2} \right], \quad (3)$$

where A is a normalization constant, and w ($\log t_1$) is the half-width at half-maximum (a central value) [16]. The Lorentzian fit can account for our observed $\Delta P(t)$ behaviors quite well.

We applied the Lorentzian fit to all of the other experimental $\Delta P(t)$ data. As shown by the solid lines in Figs. 1(c) and (d), the Lorentzian fit provides excellent explanations. Figure 3(a) presents the Lorentzian distribution

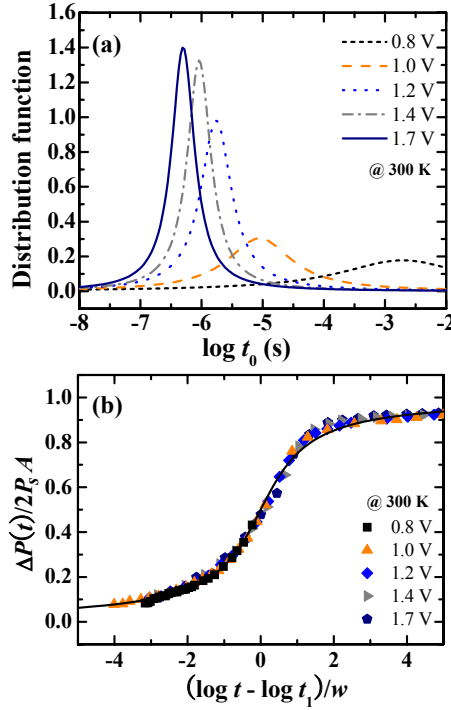


FIG. 3: (color online). (a) The E_{ext} -dependent Lorentzian distribution functions at room temperature. (b) Rescaled $\Delta P(t)$ using fitting parameters for the Lorentzian distribution function.

functions used for the 300 K data. As V_{ext} increases, $\log t_1$ and w decrease. We rescaled the experimental $\Delta P(t)/2P_s$ data using $(\log t - \log t_1)/w$. All the data merge into a single line, an arctangent function [16], as shown in Fig. 3(b). Although not indicated in this figure, the experimental data for all other T also merged with this line. This scaling behavior suggests that the Lorentzian distribution function for $\log t_0$ is intrinsic.

Note that $F(\log t_0)$ follows not the Gaussian distribution, but the Lorentzian distribution. For a statistically independent random process, it is a basic statistical rule that the resulting distribution should become Gaussian, regardless of the process details [17]. For example, impurities (or crystal defects) inside a real crystal result in inhomogeneous broadening of the light absorption line, which has a Gaussian line shape.

However, some studies have observed that magnetic resonance line broadening of randomly distributed dipole impurities follows the Lorentzian distribution [18]. The first rigorous theoretical result for this problem is that of Anderson, who showed that the distribution of any interaction field component in the system of dilute aligned dipoles should be Lorentzian [19, 20]. Polycrystalline FE films should contain many dipole defects that will act as pinning sites for the domain wall motion. To explain our observed Lorentzian distribution of $\log t_0$, we assume that a local field \bar{E} exists at the FE domain pinning sites

and that it has a Lorentzian distribution:

$$F(\bar{E}) = \frac{A}{\pi} \left[\frac{\Delta}{\bar{E}^2 + \Delta^2} \right], \quad (4)$$

where Δ is the half-width at half-maximum of the \bar{E} distribution function, related to the concentration of pinning sites.

In the low E_{ext} region, the domain wall motion should be governed by thermal activation process at the pinning sites. Without \bar{E} effects, thermal activation results in a domain wall speed in the form $v \propto 1/t_0 \propto \exp[-(U/k_B T)(E_0/E_{ext})]$, where U is the energy barrier and E_0 is the threshold electric field for pinned domains [21]. Since \bar{E} results in a change in the effective electric field at pinning sites, the associated t_0 can be expressed as

$$t_0 \sim \exp \left[\left(\frac{U}{k_B T} \right) \left(\frac{E_0}{E_{ext} + \bar{E}} \right) \right]. \quad (5)$$

Then, the distribution of \bar{E} results in a distribution in $\log t_0$, using the relation $F(\log t_0) = F(\bar{E}) \cdot |d\bar{E}(\log t_0)/d(\log t_0)|$. With

$$\log t_1 \approx \frac{UE_0}{k_B T} \cdot \left(\frac{1}{E_{ext}} \right) \quad (6)$$

and

$$w \approx \frac{UE_0\Delta}{k_B T} \cdot \left(\frac{1}{E_{ext}^2} \right), \quad (7)$$

we can obtain the desired Lorentzian distribution for $F(\log t_0)$, i.e., Eq. (3), from Eqs. (4) and (5).

Our experimental values for $\log t_1$ and w agree with the analytical forms. Figures 4(a) and (b) plot $\log t_1$ vs. $1/E_{ext}$ and w vs. $1/E_{ext}^2$ at various T , respectively. Both $\log t_1$ and w follow the expected E_{ext} -dependence in the low E_{ext} region. Note that Eq. (6) is consistent with Merz's law [22], which states that the current coming from FE polarization switching should have a characteristic time of $\exp(\alpha/E_{ext})$, where α is the activation field. Using this empirical law, several studies have measured α values. For example, So *et al.* reported $\alpha \approx 1700$ kV/cm for 100-nm-thick epitaxial PZT films [2], and Scott *et al.* reported $\alpha \approx 270$ kV/cm for 350-nm-thick poly-PZT films [23]. These values are consistent with our room temperature value of $UE_0/k_B T$, i.e., 1400 kV/cm.

Our model viewed the FE domain switching kinetics as domain wall motion driven by E_{ext} with a random pinning potential. In the low E_{ext} region, thermal activation at the pinning sites can be important, resulting in the so-called domain wall creep motion. Applying atomic force microscopy, Tybell *et al.* [21] and Paruch *et al.* [24] demonstrated that the domain-switching kinetics in epitaxial PZT films are governed by the domain wall creep motion. Some theoreticians studied the domain wall creep motion of an elastic string in a random potential. They found a linear increase in U with an increase in T [25]. The insets in Fig. 4(a) show that the

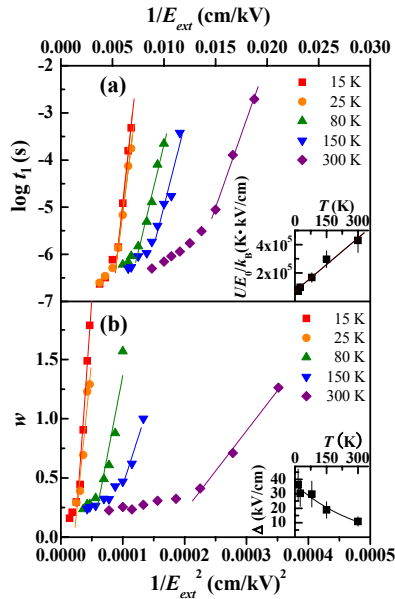


FIG. 4: (color online). E_{ext} -dependent (a) $\log t_1$ and (b) w at various T . Note that $\log t_1$ and w are proportional to $1/E_{ext}$ and to $1/E_{ext}^2$ in the low E_{ext} region, respectively. The insets show UE_0/k_B and Δ . The solid lines are guidelines for eyes.

value of UE_0/k_B obtained from the linear fits in Fig. 4(a) increase linearly with T , consistent with the theoretical prediction for U [25]. The inset in Fig. 4(b) shows Δ obtained from the fits to Fig. 4(b). Similar exponential decay behavior was predicted in a magnetic resonance study of randomly distributed dipoles [26].

At this point, we wish to compare our model with the NLS model. Although both models use Eq. (2), the origins and forms for $F(\log t_0)$ are quite different. In the NLS model, the FE film consists of numerous areas, each with its own and independent t_0 . Subsequently, it was suggested that the individually switched regions correspond to single grains or clusters of grains in which the grain boundaries act as frontiers limiting the propagation of the switched region [8]. Consequently, the NLS model can be applied for polycrystalline films only, and the form of $F(\log t_0)$ should depend on their microstructure. Conversely, in our model, the interaction between dipole defects inside the FE film induces a distribution in the local field, which results in $F(\log t_0)$. Therefore, both point defects and the grain boundaries could act as pinning sites. Using the Lorentzian distribution for $F(\log t_0)$, our model can be used for both epitaxial and polycrystalline FE films [2]. Using Eqs. (2) and (3) with small w values, we could successfully explain the $\Delta P(t)$ for FE single crystals or epitaxial thin films [2]. We also found that our model can explain the $\Delta P(t)$ data for poly-PZT films with Ti concentrations of 0.48 and 0.65.

Note that our model for thermally activated domain switching kinetics can be viewed as the famous problem that treats the propagation of elastic objects driven

by an external force in presence of a pinning potential [21, 24, 25]. It can be applied to many FE films, since the domain wall motion with a disordered pinning potential should be the dominant mechanism for $\Delta P(t)$. Therefore, the $\Delta P(t)$ studies can be used to investigate numerous intriguing issues concerning nonlinear systems, such as creep motion, avalanche phenomenon, pinning/depinning transition, and so on.

In summary, we investigated the polarization switching behaviors of (111)-oriented poly-PZT films and found that the characteristic switching time obeyed the Lorentzian distribution. We explained this intriguing phenomenon by introducing the local electric field due to the defect dipole.

The authors thank D. Kim for fruitful discussions. This study was financially supported by Creative Research Initiatives (Functionally Integrated Oxide Heterostructure) of MOST/KOSEF.

* Electronic address: twnoh@snu.ac.kr

- [1] *Ferroelectric Memories*, edited by J. F. Scott (Springer-Verlag, Berlin, 2000).
- [2] Y. W. So *et al.*, *Appl. Phys. Lett.* **86**, 92905 (2005) and references therein.
- [3] O. Lohse *et al.*, *J. Appl. Phys.* **89**, 2332 (2001).
- [4] A. K. Tagantsev *et al.*, *Phys. Rev. B* **66**, 214109 (2002).
- [5] I. Stolichnov *et al.*, *Appl. Phys. Lett.* **83**, 3362 (2003).
- [6] A. Gruverman *et al.*, *Appl. Phys. Lett.* **87**, 082902 (2005).
- [7] V. Shur *et al.*, *J. Appl. Phys.* **84**, 445 (1998).
- [8] I. Stolichnov *et al.*, *Appl. Phys. Lett.* **86**, 012902 (2005).
- [9] B. H. Park *et al.*, *Nature* **401**, 682 (1999).
- [10] N. Kolmogorov, *Izv. Akad. Nauk. Ser. Math.* **3**, 355 (1937).
- [11] M. Avrami, *J. Chem. Phys.* **8**, 212 (1940).
- [12] If all nuclei of opposite polarization arise through whole process, n could be larger than the actual dimension.
- [13] Y. S. Kim *et al.*, *Appl. Phys. Lett.* **86**, 102907 (2005).
- [14] J. Y. Jo *et al.*, *Phys. Rev. Lett.* **97**, 247602 (2006).
- [15] Complications can occur due to charge trapping or domain pinning, called the imprint effect. Refer to Ref. [1]. To prevent the imprint effect, we applied a pulse with the opposite polarity at the end of each pulse train measurement (i.e., after pulse A2).
- [16] A double exponential function $\exp[-\{10^{\log t}/10^{\log t_0}\}^n]$ with $n > 1$ can be approximated as a step function centered at $\log t_0 = \log t$. As a result, Eq. (2) can be approximated as $2P_s A/\pi \cdot [\arctan\{(\log t - \log t_1)/w\} + \pi/2]$.
- [17] F. Reif, *Fundamentals of Statistics and Thermal Physics* (McGraw-Hill, Singapore, 1985).
- [18] J. H. V. Vleck, *Phys. Rev.* **74**, 1168 (1948).
- [19] P. W. Anderson, *Phys. Rev.* **82**, 342 (1951).
- [20] J. R. Klauder and P. W. Anderson, *Phys. Rev.* **125**, 912 (1962).
- [21] T. Tybella *et al.*, *Phys. Rev. Lett.* **89**, 097601 (2002).
- [22] W. J. Merz, *Phys. Rev.* **95**, 690 (1954).
- [23] J. F. Scott *et al.*, *J. Appl. Phys.* **64**, 787 (1998).
- [24] P. Paruch *et al.*, *Phys. Rev. Lett.* **94**, 197601 (2005).
- [25] A. B. Kolton *et al.*, *Phys. Rev. Lett.* **94**, 047002 (2005).

[26] M. W. Klein, Phys. Rev. **173**, 552 (1968).